Multiwavelength studies of H II region NGC 2467

Ram Kesh Yadav, A. K. Pandey, Saurabh Sharma, and C. Eswaraiah

Citation: AIP Conf. Proc. **1543**, 148 (2013); doi: 10.1063/1.4812609
View online: http://dx.doi.org/10.1063/1.4812609
View Table of Contents: http://proceedings.aip.org/dbt/dbt.jsp?KEY=APCPCS&Volume=1543&Issue=1
Published by the AIP Publishing LLC.

Multiwavelength Studies of H II region NGC 2467

Ram Kesh Yadav, A. K. Pandey, Saurabh Sharma and C. Eswaraiah

Aryabhatta Research Institute of Observational Sciences (ARIES), Nainital - 263129, India

Abstract. We present the multiwavelength studies of the H II region Sh2-311 to explore the effects of massive stars on low-mass star formation. In this study we have used optical ($UBVI$) data from ESO 2.2m Wide Field Imager (WFI), Near-Infrared (NIR) (JHK_s) data from CTIO 4m Blanco Telescope and archival *Spitzer* 8μm data. Based on stellar density contours and dust distribution we have divided the complex into three regions i.e., Haffner 19 (H19), Haffner 18 (H18) and NGC 2467. Using the *UBVI* data we have estimated the basic parameters of these regions. We have constructed the $(J-H)/(H-K_s)$ color-color diagram and a $J/(J-H)$ color-magnitude diagram to identify young stellar objects (YSOs) and to estimate their masses. Spatial distribution of the YSOs indicates that most of them are distributed at the periphery of the H II region and ionizing star may be responsible for the triggering of star formation at the periphery of the H II region.

Keywords: HI regions, YSOs, Spatial distribution, Star formation,Pre-main sequence stars
PACS: 97.10.Bt,

INTRODUCTION

The H II region NGC 2467 also known as Sharpless 311, located in the southern part of the constellation Puppis, contains two prominent clusters Haffner 19 (H19) and Haffner 18 (H18). The region harbours two O type and several early B type stars (Feinstein & Vazquez 1989; Moreno-Corral et al. 2005; Munari & Carraro 1996; Munari et al. 1998). The brightest star in the region HD 64315 is of the spectral type O6V. On the basis of *UBVRI* broadband photometric data Moreno-Corral et al. (2002) have reported that there are 34 B type stars in the cluster H19 with the most massive being a B1V star. They estimated the age of H19 as $\simeq$ 2 Myr. In the case of H18, Fitzgerald & Moffat (1974) and Munari et al. (1998) have reported age as 1 Myr and 2 Myr, respectively. Pismis & Moreno (1976) claimed that the entire H II region is very young with an age around 2-3 Myr. De Marco et al. (2006) used Hubble Space Telescope (HST) Advanced Camera for Survey (ACS) data to identify a large number of brightened ridges and cloud fragments in this region. The ionization front appears to be near to many of these fragments, suggesting that they have been recently broken off from the molecular cloud as they are exposed to advancing ionization front. Snider et al. (2009) extensively studied the region using *Spitzer* data and suggested an ionization front with a preceding shock as the most likely triggering mechanism of star formation.

In this paper we have used deep $UBVI$, and JHK_s data to estimate reddening, and distances, as well as to identify the YSOs and to study spatial distribution of the YSOs.

First International Conference on Chemical Evolution of Star Forming Region and Origin of Life
AIP Conf. Proc. 1543, 148-156 (2013); doi: 10.1063/1.4812609

THE DATA

The data used in this study is a combination of optical ($UBVI$), NIR (JHK_s) and mid-infrared *Spitzer* 8 μm.

We have used archival optical observations which consist a set of 39 images in $UBVI$ filters taken from the WFI camera mounted at the Cassegrain focus of the ESO/MPG 2.2m Telescope at La Silla (Chile). This instrument consists of a 4 x 2 mosaic of CCDs of 2048 x 4096 pixels with a scale of 0.238 arcsec/pixel. Each chip covers an area of 8.12 x 16.25 square arcmin, while the full field of view (FOV) is 34 x 33 square arcmin. The observations were retrieved from the ESO Science Archive Facility. These observations were made during October 29 to December 07, 2002 in a service mode. The observations were carried out under slightly variable seeing conditions with full width half maximum (FWHM) of the point-spread function (PSF) varying from 0.81 to 1.69 arcsec.

Pre-processing of the optical data has been carried out using the MSCRED package (Francisco Valdes, 1998)[1] in IRAF using the standard procedure. Details about the MSCRED package can be found on IRAF help page[2]. Photometry was performed using the DAOPHOT package in IRAF. Because of source confusion and nebulousity within the NGC 2467 region, photometry was performed using PSF algorithm ALLSTAR in DAOPHOT package (Stetson 1987). The Landolt standard fields (SA98, and SA113, Landolt 1992) were observed in order to convert the instrumental magnitudes to standard magnitudes.

The deep NIR observations of the central region of Sh2-311 were obtained using the ISPI camera on CTIO 4m Blanco Telescope[3]. The ISPI is a 2048×2048 HgCdTe array having a 10.′5 square field of view (van der Bliek et al. 2004). Other details of the instrument can be found on ISPI homepage[4]. We observed the Sh2-311 region with the $J(\lambda = 1.25\mu\text{m})$, $H(\lambda = 1.63\mu\text{m})$ and $K_s(\lambda = 2.17\mu\text{m})$ filters on March 03, 2010. Stars brighter than 11 mag were saturated in the CTIO observations and were taken from the 2MASS catalogue (Cutri et al., 2003). We obtained 9 dithered exposures (60 sec) of the target centered at $(\alpha, \delta) = (07^h52^m23^s.555, -26^o24'54.66'')$ (J2000) simultaneously for each band. Fig. 1 shows the K_s band image of the NGC 2467 region. The area on the lower left and lower right of the image (cf. Fig. 1) marked with a box are used as a reference field to estimate the field star contamination. Instrumental magnitudes were obtained using the same procedure followed for the optical data. The instrumental magnitudes were calibrated using the 2MASS data. The data were then converted to the California Institute of Technology (CIT) system using the color transformation equations given by Carpenter (2001). The *Spitzer* 8 μm image has been used to trace the interaction of expanding H II region with the adjacent molecular cloud.

---

[1] http://www.ast.cam.ac.uk/ rgm/scratch/e.eglez/iraf/mscguide.txt
[2] http://iraf.noao.edu/projects/ccdmosaic/mscguide.html
[3] http://www.ctio.noao.edu/noao/content/victor-blanco-4-m-telescope
[4] http://www.ctio.noao.edu/noao/content/ispi

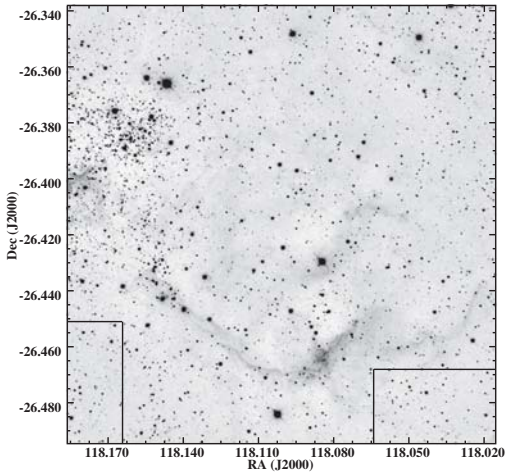

FIGURE 1. CTIO K_s-band image of NGC 2467 region. Lower-left and lower-right boxes represents the regions selected as reference fields.

RESULTS AND DISCUSSIONS

Stellar density distribution

Fig. 2 shows the isodensity contours (thick black curves) generated from the 2MASS K_s-band data (with $\sigma_{K_s} < 0.1$ mag) using a grid size of $\simeq 36$ arcsec. The contours are plotted above 1σ level. The contours have step size of 2 stars/arcmin^2 with the lowest contour representing 13 stars/arcmin^2. The stellar isodensity contours manifest two prominent clustering in the region . The *Spitzer* 8 μm isointensity contours (blue contours) are also over-plotted in Fig. 2. On the basis of stellar density and 8 μm emission distributions we have selected three regions, namely H19 (top-left circle), H18 (central circle) and NGC 2467 (bottom-right circle) for a detailed study.

Reddening and Distance to the clusters

The extinction towards star forming regions (SFRs) or star clusters arises due to two distinct sources: (1) the general interstellar medium in the foreground of the region $[E(B-V)_{min}]$, and (2) the localized cloud associated with the region $[E(B-V)_{local} = E(B-V) - E(B-V)_{min}]$, where $E(B-V)$ is the observed reddening of the stars embedded in the local cloud. The presence of the molecular cloud (Lada & Wooden 1979) and the nebulousity associated with NGC 2467 would give rise to a variable extinction within this region. To estimate the extinction towards the regions, we used the $(U-B)/(B-V)$ two colour diagram (TCD) (see Sharma et al., 2007). Fig. 3 (left two panels) shows the $(U-B)/(B-V)$ TCD for the stars in H19 and H18 regions, respectively. Minimum reddening values for H19 and H18 are found to be 0.40 mag and 0.55 mag, respectively. In the case of NGC 2467 region only a few bright stars could be detected in optical pho-

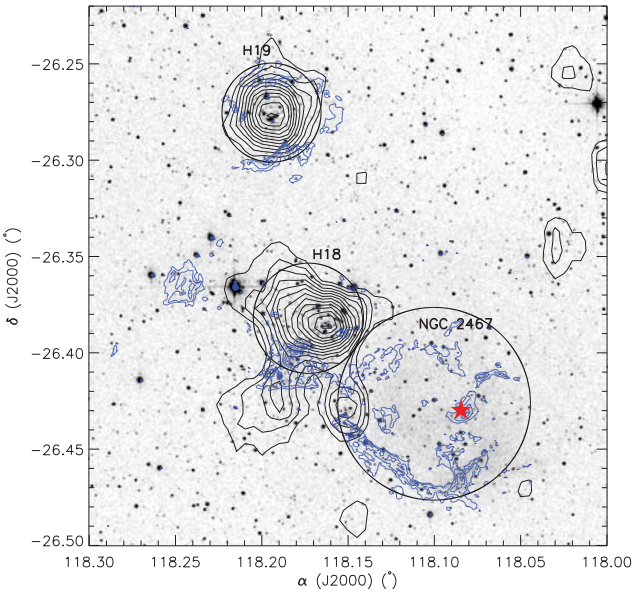

FIGURE 2. 2MASS K_s-band 30 × 30 square arcmin image of NGC 2467. Black contours represent the stellar surface density distribution. Blue contours represent the Spitzer 8μm isointensity distribution. H19, H18 and NGC 2467 regions are also shown by black circles (top-left, middle, and bottom-right, respectively). Most massive O6 star is shown with red star.

tometry, so we have used the NIR TCD (Fig. 3; right panel) to estimate the extinction in the region. The A_V values for individual stars were estimated by tracing back the NIR excess stars to the T-Tauri locus, which is described in next section. The mean A_V for the region comes out to be 1.24 which corresponds $E(B-V) = 0.40$ mag.

The $V/(V-I)$ color-magnitude diagrams (CMDs) shown in Fig. 4 have been used to estimate the distance to clusters. The zero-age main sequence (ZAMS) by Marigo et al. (2008) for the solar metallivity ($Z = 0.02$) was visually fitted to the observed data using the $E(B-V)_{min}$ values for the individual regions. The distances to the clusters H19, H18, and NGC 2467 are found to be 5.6 kpc, 5.0 kpc and 5.3 kpc, respectively.

NIR TCD: Identification of YSOs

The present deep NIR photometry detects a total of 9119, 9365 and 10294 sources in J, H and K_s bands, respectively. We prepared catalog of 4457 sources common in all the three bands having errors in each band less than 0.1. Fig. 5 (left panel) shows the $(J-H)/(H-K_s)$ TCD for all the 4457 sources in the region as well as for the sources located in the reference field (right panel).The solid and thick dashed curves represent the unreddened main-sequence (MS) and giant branch (Bessell & Brett 1988). The parallel dashed lines are the reddening vectors for early- and late-type stars (drawn from the base and tip of the two branches). The dotted line indicates the locus of T-Tauri stars (Meyer, Calvet & Hillenbrand 1997). The extinction ratio $A_J/A_V = 0.265$, A_H/A_V=0.155

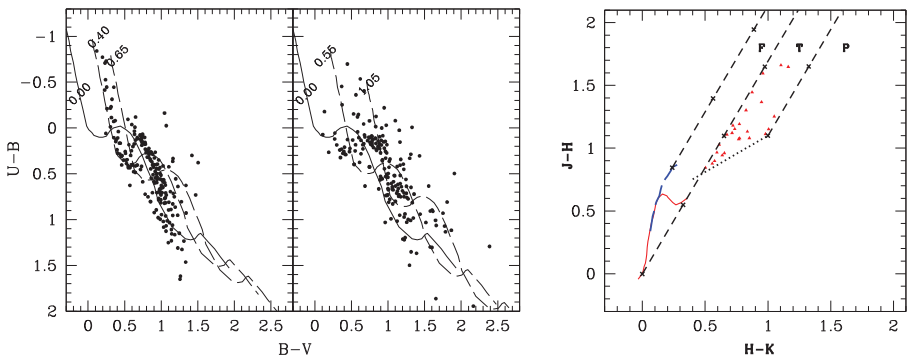

FIGURE 3. Left:$(U-B)/(B-V)$ color-color diagrams of stars in H19 and H18 regions. The continuous curve represents intrinsic MS by Schmidt-Kaler (1982) shifted along the reddening vector of 0.72 for E(B - V) = 0.40 mag for H19 and E(B - V) = 0.55 mag for H18. Right: $(J-H)/(H-K_s)$ color-color diagram for the NIR excess sources in the NGC 2467 region. The continuous line marks the locus of MS and the thick dashed line is the locus of giant stars . The three parallel dashed lines represent the reddening vectors with crosses speprated by a visual extinction of A_V = 5 mag.

and A_{K_s}/A_V=0.090 have been taken from Cohen et al. (1981). We classified the sources into three regions in the statistically cleaned TCD (cf. Ojha et al. 2004a, and references therein). 'F' sources are located between the reddening vectors projected from the intrinsic color of MS stars and giants and are considered to be the field stars (MS stars, giants) or Class III/Class II sources with small NIR excesses. 'T' sources are located redward of the region 'F' but blueward of the reddening line projected from the red end of T Tauri locus of Meyer et al. (1997). These sources are considered as classical T Tauri stars (Class II objects) with large NIR excesses. There may be an overlap in NIR colors of Herbig Ae/Be stars and T Tauri stars in the 'T' region (Hillenbrand et al. 1992). 'P' sources are those located in the region redward of the region 'T' and are most likely Class I objects (protostar-like objects; Ojha et al. 2004b). Comparison of the $J-H/H-K_s$ TCDs of the NGC 2467 region and of the reference field suggests that the sources exhibiting NIR excess emission (i.e., located in the the 'T' region of the TCD) could be the YSOs associated with the region.

Fig. 6 shows $J/(J-H)$ CMD for all 4457 sources detected in the region (black dots) along with the 156 identified YSO candidates (red open circles). The post main-sequence isochrones (black curve) for 1 Myr (Z=0.02) by Marigo et al. (2008) has been plotted correcting for the distance and reddening. The PMS isochrones (blue curve) for 1 Myr is taken from Siess et al. (2000) The continuous oblique reddening lines denote the positions of 1 Myr PMS stars having masses between $0.16M_\odot$ - $4.0M_\odot$.

Spatial Distribution of YSOs

Fig. 7 shows that majority of the YSOs are distributed at the periphery of HII region NGC 2467. In Fig. 2 we have over-plotted the 8.0μm emission contours. The *Spitzer* –

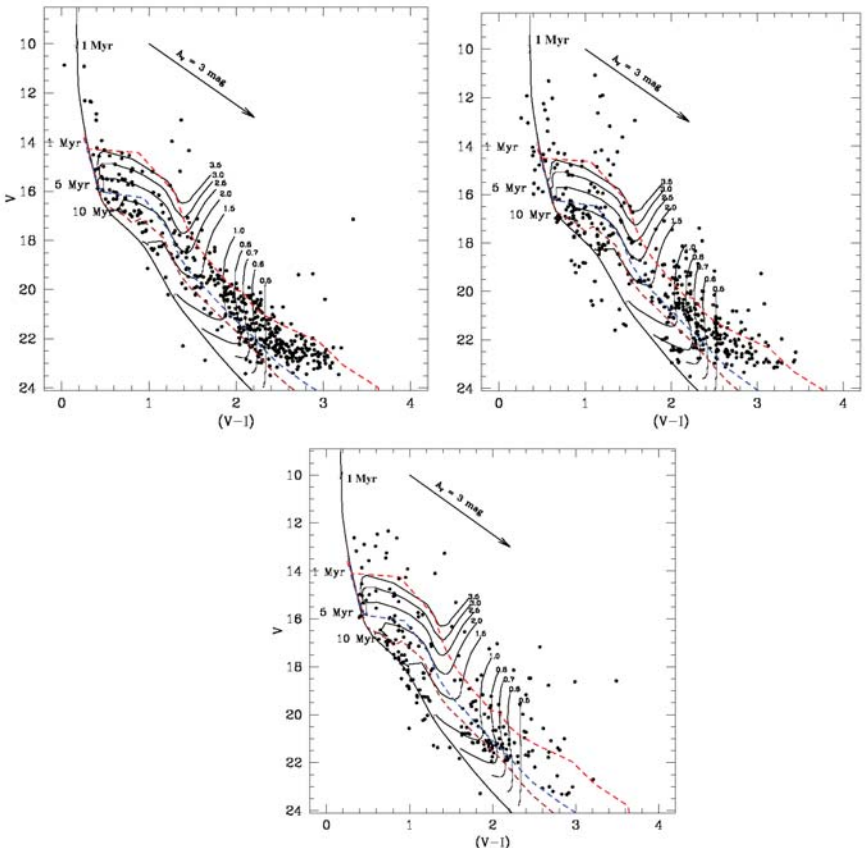

FIGURE 4. $V/(V-I)$ statistically cleaned CMD for the member star of H19 (top-left), H18 (top-right), and NGC 2467 (bottom), respectively. Continuous line represents 1 Myr isochrone taken from Marigo et al. (2008), and dashed curves represent PMS isochrones for 1 Myr, 5 Myr and 10 Myr by Siess et al. (2000) (dashed lines). All the isochrones are corrected for the respective distance and reddening towards the clusters. Evolutionary tracks for diferrent masses are also shown.

IRAC Ch3 is centered on 8.0 μm which also contains the 7.7 μm and 8.6 μm emission bands generally attributed to the poly-cyclic aromatic hydrocarbon (PAH) molecules. Infrared emission from PAHs is observed in the photo-dissociation regions (PDRs), which generally traces the interaction of expanding H II regions with molecular clouds. Fig. 7 shows that majority of the YSOs are distributed at the periphery of H II region.

Conclusions

Using the deep optical and NIR photometry we have estimated the extinction and distance to the clusters associated with the region. The extinction towards the clusters is found to be variable. The distance to the clusters H19, H18, and NGC 2467 is found to be 5.6 kpc, 5.0 kpc, and 5.3 kpc, respectively. Our NIR TCD yield 156 YSOs with NIR

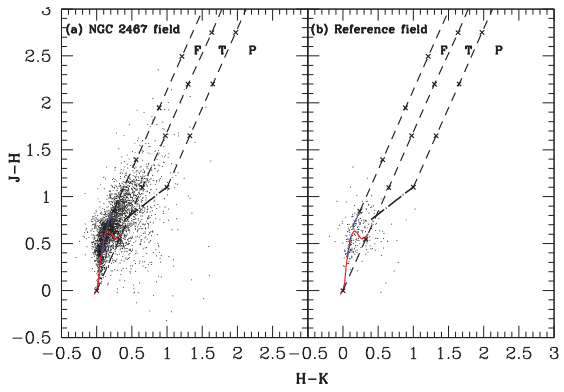

FIGURE 5. $(J-H)/(H-K_s)$ TCD for all the sources detected in NGC 2467 region (a) and for the reference field (b). The continuous line marks the locus of MS and the thick dashed line is the locus of giant stars (Bessell & Brett, 1988). The dotted line indicates the locus of unreddened CTTSs (Meyer et al., 1997). The three parallel dashed lines represent the reddening vectors with crosses representing a visual extinction of A_V = 5 mag.

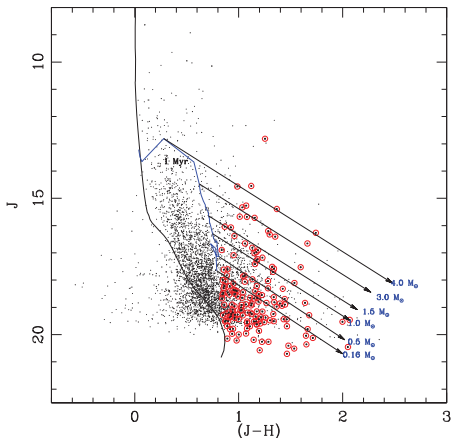

FIGURE 6. $J/(J-H)$ CMD for all the stars (black dots) within NGC 2467 region along with the identified NIR excess sources (open circles). The isochrone of 2 Myr (Z=0.02) and PMS isochrones of age 1 and 10 Myr by Marigo et al. (2008) and Siess et al. (2000), respectively, corrected for a distance and reddening . The parallel slanting lines denotes loci of 1 Myr old PMS stars having masses in the range of 0.16 $M_\odot$ - 4.0 $M_\odot$ taken from Siess et al. (2000).

excess suggesting an on-going star-formation in the Sh2-311 region. Spatial distribution of YSOs indicates that the majority of the YSOs are found to be preferentially distributed at the eastern border of Sh2-311. The *Spitzer* 8 μm emmission and distribution of YSOs suggest that the region is quite young and an important site for studying the star formation activity.

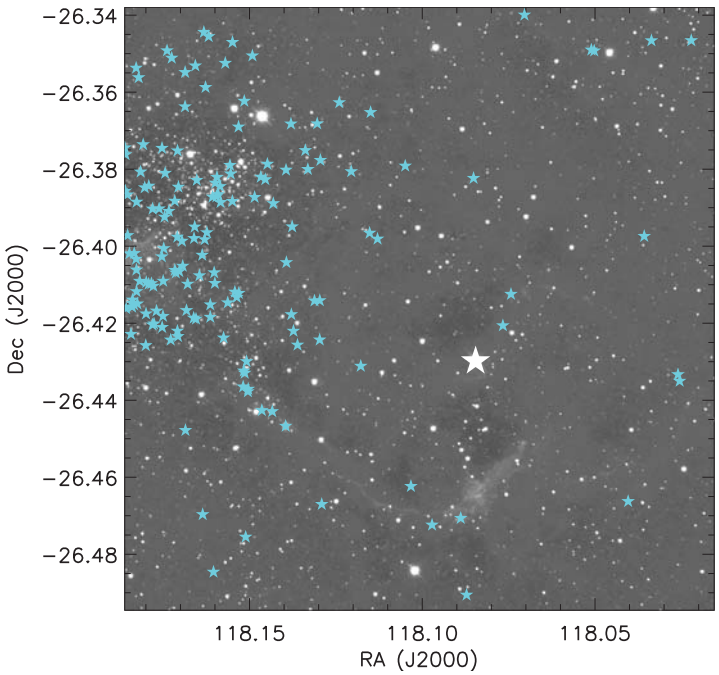

FIGURE 7. NIR-excess source distribution (cyan stars) overlaid on the K_S-band grey-scale image. Most massive O6 star is shown with big white star.

ACKNOWLEDGMENTS

This study makes use of data from Two Micron All Sky Survey and Spitzer space telescope. The WFI observations used in the present work have been taken from the VLT archive. The authors are thankful to Prof. Frank Valdes for help during WFI data reduction.

REFERENCES

1. De Marco, O., et al. 2006, *AJ*, 131, 2580
2. Feinstein, A., & Vázquez, R. A. 1989, *A&AS*, 77, 321
3. Fitzgerald, M. P., & Moffat, A. F. J. 1974, *AJ*, 79, 876
4. Moreno-Corral, M. A., Chavarrì, a-K. C., & de Lara, E. 2002, *RevMexAA*, 38, 141
5. Munari, U., Carraro, G., & Barbon, R. 1998, *MNRAS*, 297, 867
6. Pandey A. K. et al. 2005, *MNRAS*, 358, 1290
7. Pismis, P., & Moreno, M. A. 1976, *RevMexAA*, 1, 373
8. Cutri R. M. et al., 2003, 2MASS All-Sky Catalog of Point Sources. NASA/IPAC Infrared Science Archive (online-only reference): http://irsa.ipac.caltech.edu/applications/Gator
9. Stetson P. B., 1987, *PASP*, 99, 191
10. Carpenter J. M., 2001,*AJ*, 121, 2851
11. Lada C. J., Wooden D., 1979, *ApJ*, 232, 158
12. Girardi L. et al., 2002, *A&A*, 391, 195
13. Bessell, M. S., & Brett, J. M. 1988, *PASP*, 100, 1134

14. Hillenbrand, L. A., Strom, S. E., Vrba, F. J., & Keene, J. 1992, *ApJ*, 397, 613
15. Landolt, A. U. 1992, *AJ*, 104, 340
16. Marigo, P. et al., 2008, *A&A*, 482, 883
17. Meyer, M., Calvet, N., & Hillenbrand, L. A. 1997, *AJ*, 114, 288
18. Ojha, D. K. et al., 2004a, *ApJ*, 608, 797
19. Ojha, D. K. et al., 2004b, *ApJ*, 616,1041
20. Sharma, Saurabh et al., 2007, *MNRAS*, 380, 1141
21. Schmidt-Kaler, Th. 1982, *Landolt-Bornstein*, Vol. 2b, ed. K. Schaifers, H. H. Voigt & H. Landolt (Berlin: Springer), 19
22. Siess L., Dufour E., Forestini M., 2000, *A&A*, 358, 593
23. Snider, Kelly D. et al. 2006, *ApJ*, 2009, 700, 506
24. van der Bliek, N. S., et al. 2004, *Proc. SPIE*, 5492, 1582